ACS Sustainable Chemistry & Engineering

pubs.acs.org/journal/ascecg

Research Article

Sustainable Open Production of *Short–Medium*-Chain Length Polyhydroxyalkanoates from Crude Glycerol in Batch and Fed-Batch Bioreactors by *Pseudomonas frigusceleri* MPC6

Matias Orellana-Saez, Izabook Gutierrez-Urrutia, Fabian Rodriguez-Oyarzo, Benjamin Cordero-Jorquera, Andrea Carvajal, Eduardo Castro-Nallar, Cesar Saldias, Esteban A. Hernandez-Vargas, Virginia Rivero-Buceta, Flavia C. Zacconi, and Ignacio Poblete-Castro*

Cite This: https://doi.org/10.1021/acssuschemeng.5c03946

Read Online

ACCESS | Metrics & More | Article Recommendations | Supporting Information

ABSTRACT: Nonsterile microbial synthesis of chemicals offers a promising route to reducing production costs and establishing sustainable processes. Here, we investigated polyhydroxyalkanoate (PHA) production from glycerol by different *Pseudomonas* strains under nonsterile conditions at varying NaCl concentrations. There was a negative correlation between PHA synthesis and increasing salt levels for *P. putida* H and KT2440. In contrast, *P. frigusceleri* MPC6 exhibited, for the first time, enhanced PHA production on glycerol in the presence of 20 g L^{-1} NaCl. In open-batch bioreactors, the strain MPC6 produced 0.03 g L^{-1} h^{-1} PHA (42 wt%) from crude glycerol and remained the dominant member of the bacterial community (>98%). We then developed a nonsterile fed-batch process that achieved 52.5 g L^{-1} of total biomass using a carbon-limiting feeding scheme. A DO-stat feeding approach during nitrogen limitation resulted in a PHA volumetric productivity of 0.47 g L^{-1} h^{-1} with PHA comprising 45% of the biomass. The major monomer in the polymeric chain was 3-hydroxybutyrate (PHB, 87–89%), with the remainder as *mcl*-PHA. This study demonstrates that halotolerant bacteria can produce high levels of biopolymers under mild salinity conditions that are less corrosive than those in high-salt systems while avoiding sterilization steps, thereby lowering the operating costs of the bioprocess.

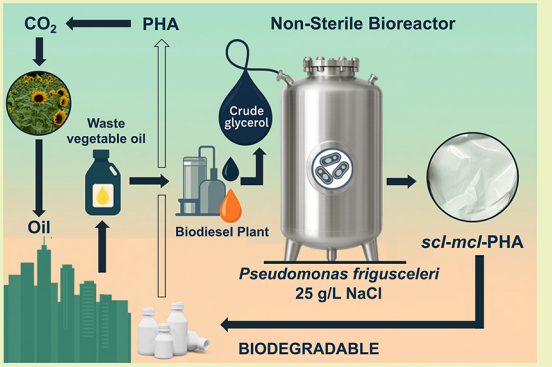

KEYWORDS: *polyhydroxyalkanoates, crude glycerol, nonsterile fed-batch bioreactors, halotolerant, Pseudomonas frigusceleri MPC6*

1. INTRODUCTION

Polyhydroxyalkanoates (PHAs) represent a family of biodegradable polymers synthesized by bacteria and archaea through the fermentation of renewable materials. PHAs display similar properties to petrochemical plastics such as polypropylene and polystyrene, which are used in the agro-industrial, medical, and packaging sectors.[1] Despite these benefits, PHAs are expensive to produce due to the high cost of carbon substrates and fermentation settings.[2,3] Research has focused on using low-cost feedstocks[4] to derive PHAs including waste fatty acids,[5] lignin,[6,7] and crude glycerol[8] from the biodiesel industry to circumvent these hurdles. Moreover, the supplementation of NaCl (2–10% w/v) to the fermentation media allows the operation of bioreactors under nonsterile conditions using halophilic bacteria and archaea, especially the native PHA-producing *Halomonas*, *Haloferax*, and *Bacillus* species.[9,10]

In the past decade, there has been an ongoing effort to bioconvert crude glycerol, a side-product generated from the esterification process of fatty acids in the biodiesel industry, into biobased chemicals[11] given its low cost and a high degree of reduction.[8] Unfortunately, crude glycerol contains many growth-inhibitory compounds including salt, heavy metals, ashes, and methanol.[11,12] In this regard, bacteria of the genus *Pseudomonas* can cope with these adverse conditions[8] and have proven to be suitable *medium-chain* length PHA (*mcl*-PHA) production platforms[13] in batch[14,15] and fed-batch processes.[16–18] However, no *Pseudomonas* strains have been shown to maintain good biomass and PHA accumulation yields when challenged with NaCl concentrations sufficient to suppress the growth of competing microorganisms. Moreover, the homopolymer PHB and the less-brittle copolymer PHBV have also been produced from crude glycerol, with a high PHBV volumetric productivity observed only when the waste glycerol was supplemented with yeast extract.[19]

Received: April 27, 2025
Revised: September 11, 2025
Accepted: September 11, 2025
Published: September 29, 2025

To truly harness NaCl-supplemented media as a selective barrier to avoid energy-intensive steam sterilization of vessels and bioreactors to reduce the operational costs, we must identify novel bacterial strains that sustain growth and high-level PHA accumulation at NaCl concentrations sufficient to suppress contamination. In this study, we selected *P. frigusceleri* MPC6,[20,21] an Antarctic halotolerant bacterium,[22] and compared it with two established PHA-producing *Pseudomonas* strains; the model *Pseudomonas putida* KT2440,[15] which proliferates on crude glycerol,[16] and *Pseudomonas putida* H,[23] a robust PHA producer able to cope with the high toxicity of aromatic compounds derived from lignin hydrolysis.[6] All *Pseudomonas* strains were challenged to grow and accumulate PHA at increasing NaCl concentrations in batch cultures.

The novelty of this study lies in what is, to our knowledge, the first demonstration of a *Pseudomonas* strain exhibiting improved PHA synthesis under osmotic stress, with *P. frigusceleri* MPC6 being the best PHA producer and dominating the bacterial community when cultured in nonsterile bioreactors fed solely with untreated crude glycerol. We also show that *P. frigusceleri* in open fed-batch bioreactors reached the highest *short-* and *medium*-chain length PHA volumetric productivity so far reported using crude glycerol, displaying desired physical properties for industrial applications.

2. EXPERIMENTAL SECTION

2.1. *Pseudomonas* Strains. *P. putida* KT2440 (DSM 6125) was obtained from the DSMZ collection, Germany, *P. putida* H was kindly provided by Prof. Dietmar Pieper from HZI, Germany, and *P. frigusceleri* MPC6 (RGM3289) was obtained from the Chilean Collection of Microbial Genetic Resources, INIA. These bacteria were used for the different shaking flask experiments and the MPC6 strain for PHA synthesis in bioreactor.

2.2. Culture Conditions in Shake Flask Experiments. *Pseudomonas* strains were stored in 25% glycerol at − 80 °C as glycerol stocks. Cells were routinely streaked on Lysogenic broth (LB) agar plates and grown overnight to isolate single colonies. For any shake flask cultivation, *P. putida* strains were aerobically grown at 30 °C. Single colonies were picked from the plate and transferred into a 50 mL shake flask containing 10 mL of LB liquid medium. Defined minimal medium (M9) containing 4 (g L^{-1}) crude glycerol. The crude glycerol was not treated or modified in any way. It was supplied by Cremer Oleo GmbH, (Hamburg, Germany, https://www.cremeroleo.de/) and was used for all the experiments unless otherwise stated. The company also provided the technical composition of the crude glycerol, which contains (w w^{-1}) 80% glycerol, 0.5% methanol, 10% ash, 3% organic matter, and 6.5% water. We independently verified the glycerol concentration via HPLC as described below.

Bacteria were grown in M9 minimal medium[24] consisted (per liter) of 12.8 g $Na_2HPO_4{\cdot}7H_2O$, 3 g KH_2PO_4, 1 g NH_4Cl, and 0.5 g NaCl. After autoclave sterilization, the medium was supplemented with filtered trace elements (6.0 $FeSO_4{\cdot}7H_2O$, 2.7 $CaCO_3$, 2.0 $ZnSO_4{\cdot}H_2O$, 1.16 $MnSO_4{\cdot}H_2O$, 0.37 $CoSO_4{\cdot}7H_2O$, 0.33 $CuSO_4{\cdot}5H_2O$, and 0.08 H_3BO_3 (mg L^{-1})) and 0.12 g of $MgSO_4{\cdot}7H_2O$. Ten milliliters of M9 medium in a 50 mL shake flask was inoculated with the overnight LB-grown culture at an initial OD at 600_{nm} of 0.2 and incubated overnight. A second preculture was initiated by transferring a predetermined volume of the previous one into 150 mL of M9 medium containing 4 g L^{-1} pure or crude glycerol (C/N ratio = 7.0 mol mol^{-1}) in 500 mL Erlenmeyer flasks and, it was incubated overnight. At this C/N ratio, nitrogen is in excess and PHA formation is not induced.[15,20]

2.3. Batch Bioreactors for PHA Production under Axenic and Nonsterile Conditions. Batch bioreactors were operated under aerobic conditions with a working volume of 0.8 L in a 1-L Minifors2 bioreactor (INFORS HT, Switzerland) set at 30 °C. The stirring speed was kept constant at 800 rpm, and the pH was maintained at 6.8 by automatic pH-controlled addition of 1 M NaOH. The aeration rate was set at 0.8 L min^{-1} using a mass flow controller to ensure that the dissolved oxygen was above 30% of air saturation.

For the open batch bioreactors, the salts of the M9 medium were added into a clean vessel and dissolved in distilled water together with 25 g L^{-1} NaCl, followed by nonsterile 30 g L^{-1} (pure or crude glycerol) and mixing at 500 rpm. Once the solution was homogeneous, magnesium sulfate (0.12 g L^{-1}) and 0.8 mL of 1,000X nonsterile trace element solution were added. The nonsterile bioreactor was then inoculated at an initial cell density of 0.05 g L^{-1} (~0.1 OD_{600}) at a working volume of 800 mL. The C/N ratio of 17.2 mol mol^{-1} was chosen because this condition promotes PHA synthesis in *Pseudomonas*, as reported previously.[15,25] Upon completion of the run, the culture broth was removed and the bioreactor rinsed with distilled water before the next run. For the sterile batch bioreactors, the vessel containing M9-salt medium and 30 g L^{-1} (pure or crude glycerol) was autoclaved. After cooling, filter-sterilized magnesium sulfate and trace elements were added aseptically. The axenic bioreactor was then inoculated at the same initial cell density as the nonsterile bioreactor. Each bioreactor was performed in triplicates.

2.4. Unsterile Open Fed-Batch Process Using Crude Glycerol for PHA Biosynthesis. The vessels of the unsterile open fed-batch processes were previously rinsed with distilled water only. The fed-batch reactor contained nonsterile M9 medium supplemented with 15 g L^{-1} crude glycerol, 25 g L^{-1} NaCl, 0.12 g L^{-1} $MgSO_4{\cdot}7H_2O$, 2 mL of trace element solution, and 0.1 mL of Tego Antifoam 2290 (APEO-free based on paraffinic oil, Evonik, Germany). An initial working volume of 0.5 L was prepared in a 2 L vessel (Minifors2, INFORS HT, Switzerland) for the fermentation processes. The temperature was maintained at 30 °C and the airflow rate was set at 1 L min^{-1} of compressed air. For pH control, 12.5% (w v^{-1}) NH_4OH was added as needed to stabilize the pH to 6.8 ± 0.1 during the biomass formation phase, while also serving as a nitrogen source to prevent nitrogen limitation. During the PHA production phase, NH_4OH was replaced with 10% (w v^{-1}) NaOH.

The process initiated by seeding the reactor with the second preculture to achieve an initial cell concentration of 0.1 g L^{-1}. During the biomass production phase (stage II), the airflow rate was maintained at 1 L min^{-1}, with an air-to-pure oxygen ratio of 10:1. Two additional pulses of Tego Antifoam 2290 during the exponential feeding phase were provided, each of 100 μL. In the PHA production phase, the airflow rate was maintained, but pure oxygen was discontinued, and the reactor was sparged solely with compressed air. This adjustment improved the dissolved oxygen (DO) response during carbon substrate feeding.

The agitation speed was automatically adjusted to 1,200 rpm to maintain dissolved oxygen levels above 20% air saturation. The feeding nonsterile solution consisted of 500 g L^{-1} crude glycerol, 25 g L^{-1} NaCl, and 12 g L^{-1} $MgSO_4{\cdot}7H_2O$. An exponential feeding strategy was employed during the biomass production phase to maintain μ to a desirable constant μ_{set} at nearly quasi steady-state of the substrate concentration (S, g L^{-1}) in the broth, where the derivation of the feed profile followed the mass balances of the fed-batch operation.

$$F(t) = \frac{dV}{dt} \tag{1}$$

where $F(t)$ represents the feed rate (L h^{-1}), V is the culture volume (L), t is the time elapsed after the start of feeding (h).

The biomass balance is:

$$\frac{d(XV)}{dt} = \mu XV \tag{2}$$

where X is the biomass concentration (g L^{-1}), μ is the specific growth rate (h^{-1}), and integration yields:

$$X(t)V(t) = X_0V_0e^{(\mu set \cdot t)} \tag{3}$$

https://doi.org/10.1021/acssuschemeng.5c03946
ACS Sustainable Chem. Eng. XXXX, XXX, XXX−XXX

The substrate (glycerol) balance is:

$$\frac{d(SV)}{dt} = F(t)S_0 - \frac{\mu XV}{Y_{xs}} \quad (4)$$

where S (g L^{-1}) is the substrate concentration in the broth, S_0 (g L^{-1}) is the substrate concentration in the feed, Y_{xs} the biomass yield on substrate (gX gS^{-1}). Under exponential feeding to hold $\mu = \mu_{set}$ with near-zero residual substrate in the broth ($S \approx 0$), Eq. 4) reduces to,

$$\frac{XV\mu_{set}}{Y_{xs}} = F(t)S_0 \quad (5)$$

Using Eq. 3) from the biomass balance, the required feed rate is

$$F(t) = \frac{\mu_{set}X_0V_0e^{(\mu_{set}\cdot t)}}{Y_{xs}S_0} \quad (6)$$

Here, μ_{set} is the desired specific growth rate (0.75 μ_{max} = 0.12 h^{-1}), S_o (500 g L^{-1} crude glycerol), Y_{xs} (0.52 gX $gGly^{-1}$), V_0 is the culture volume (L) at the start of feeding, and X_0 (g L^{-1}) is the biomass concentration at the start of feeding.

2.5. Biomass Quantification and Analytical Procedures. Cell growth was monitored by measuring the optical density at 600 nm (OD_{600}) using a spectrophotometer (Ultraspec 2000 Hitachi, Japan). For cell dry weight (CDW) determination, 10 mL of cell culture was centrifuged at 9,000×*g* for 10 min at 4 °C. The cell pellet was washed once with distilled water and transferred to preweighed tubes. The pellet was then dried at 100 °C until a constant weight was achieved. Ammonium levels in the supernatant were quantified offline using a photometric test (LCK 303 kit, Hach Lange, Danaher, United States). The glycerol and organic acids concentration (citrate, isocitrate, succinate, fumarate, malate, pyruvate, and citrate) in cultivation supernatant was analyzed after proper dilution by HPLC ChroZen 2021 (Young Chromass, Korea) equipped with an Aminex HPX 87 H column (Biorad, Hercules, CA, USA) set at 65 °C with 0.013 N H_2SO_4 as the mobile phase (0.5 mL min^{-1}) followed by detection using a ChroZen RID detector.

2.6. PHA Characterization and Quantification. The polyesters were first subjected to methanolysis to determine the monomeric composition of PHA and the intracellular PHA content as previously described.[26] For this purpose, 10 mL of culture was transferred to a Falcon tube, and cells were harvested by centrifugation at 9,000×*g* for 10 min at 4 °C (Eppendorf 5810 R, Hamburg, Germany). The pellets were washed once with distilled water, and the supernatants were discarded. The pelleted cells were stored at − 20 °C until further analysis. The frozen cell pellets were lyophilized (Alpha LSC, Christ, Germany) at −45 °C under vacuum for 16 h. Then, 5−8 mg of dry biomass was suspended in 2 mL chloroform and 2 mL methanol containing 15% sulfuric acid, and 0.5 mg mL^{-1} 3-methylbenzoic acid and incubated at 100 °C for 4 h in sealed glass tubes. After cooling the solution, 1 mL distilled water was added and the mixture vortexed vigorously for 30 s. The mixture was centrifuged at 5,000×*g* for 10 min at room temperature, the upper phase was discarded and the lower chloroform-phase containing the methyl-ester monomers was transferred to a GC-MS vial for injection.

The methyl-esters of the monomers were analyzed using gas chromatography (GC) coupled with mass spectrometry (MS). One microliter of the organic phase was injected into a Varian GCMS system 450GC/240MS ion trap mass spectrometer (Varian Inc., Agilent Technologies) at a split ratio of 1:10. Data were processed using a MS Workstation 6.9.3 (Varian Inc., Agilent Technologies). The methyl esters of 3-hydroxybutyrate, 3-hydroxyhexanoate, 3-hydroxyoctanoate, 3-hydroxydecanoate, 3-hydroxydodecanoate, 3-hydroxy-5-cis-dodecanoate, and 3-hydroxytetradecanoate were separated using a FactorFour VF-5 ms capillary column (30 m × 0.25 mm i.d. × 0.25 mm film thickness). Calibration was performed using commercial PHB (Sigma−Aldrich, MI, United States) and purified *mcl*-PHA from a previous study.[27] Both standards were subjected to methanolysis as described above under identical conditions, and the resulting methyl-ester chromatograms were used to assign retention times and integrate the corresponding peak areas. The carrier gas, helium, was set to a flow rate of 0.9 mL min^{-1}. The injector and transfer line temperatures were maintained at 275 and 300 °C, respectively. The oven temperature was programmed as follows: 40 °C for 2 min, followed by a gradual increase to 150 °C at a rate of 5 °C min^{-1}, and finally to 280 °C at a rate of 10 °C min^{-1}. Positive ions were captured using electron ionization at 70 eV, and mass spectra were recorded by scanning ions from m/z 50 to m/z 650. The PHA concentration was determined using the method described by Lageveen and col.[26] The percentage of biopolymer relative to the cell dry weight (CDW) was calculated as the average of two or three biological replicates to determine the PHA content (wt%).

2.7. Transmission Electron Microscopy and Determination of Cellular Size. Prior to fixation, bacterial cells were cooled to 4 °C. They were then fixed with 2% glutaraldehyde and 5% formaldehyde and washed with cacodylate buffer (0.01 mol L^{-1} cacodylate, 0.01 mol L^{-1} $CaCl_2$, 0.01 mol L^{-1} $MgCl_2{\cdot}6H_2O$, and 0.09 mol L^{-1} sucrose, pH 6.9). The cells were stained for 1 h at room temperature with 1% aqueous osmium tetroxide. Dehydration was carried out using acetone at increasing concentrations (10, 30, 50, 70, 90, and 100%), with each step lasting 30 min. The 70% acetone step, which included 2% uranyl acetate, was performed overnight. Samples were infiltrated with an epoxy resin using the Spurr formula for hard resin. Ultrathin sections were cut using a diamond knife and counterstained with a mixture of uranyl acetate and lead citrate. Images were acquired using a TEM910 transmission electron microscope (Carl Zeiss, Oberkochen, Germany) operated at an acceleration voltage of 80 kV. Digital images of the ultrathin sections were captured using a Slow-Scan CCD-Camera (ProScan, 1,024 × 1,024, Scheuring, Germany) with ITEM-Software (Olympus Soft Imaging Solutions, Münster, Germany).

Digital images were retrieved and processed to precisely adjust contrast and brightness to enhance their visualization. Cell size was determined using the software ImageJ (https://imagej.net/ij/). For each condition, the size of 25 cells was measured across a total of 20 images.

2.8. FAMEs Analysis by GC-MS. The cell pellet from a 15 mL culture was transferred into a polypropylene tube. Sequentially, 4 mL of chloroform, 8 mL of methanol, and 3.2 mL of 1% NaCl were added. After each addition, the tube was vortexed vigorously for 15 s. The mixture was then agitated overnight on a tube rotator at 30 rpm. Following this, 4 mL of chloroform and 4 mL of 1% NaCl were added, and the tube was inverted 30 times to ensure thorough mixing. Phase separation was achieved by centrifugation at 4,000×*g* for 5 min at room temperature. The bottom layer, containing the lipid extract, was carefully collected and evaporated to dryness under a gentle stream of nitrogen. The dried extract was subsequently dissolved in 1 mL of a chloroform/methanol mixture (2:1, v v^{-1}). The GC-MS analysis was conducted with the same equipment as for PHA determination. The column temperature was initially held at 130 °C for 2.5 min, then increased to 240 °C at a rate of 5 °C min^{-1}, followed by a ramp to 300 °C at 30 °C min^{-1}, and finally held at 300 °C for 5 min. Additional temperature settings were as follows: inlet, 275 °C; GC-MS transfer line, 280 °C; ion source, 230 °C; and quadrupole, 150 °C. The mass-selective detector was operated in scan mode, covering a mass range of m/z 40 to 700. Compound identification was based on retention times, fragmentation patterns, and comparison with reference standards of Supelco FAME Mix (Sigma-Aldrich), and the NIST database.

2.9. Thermal Analysis of Biosynthesized PHAs. Differential Scanning Calorimetry (DSC) was employed to analyze the thermal properties of the polymer samples, including the glass transition temperature (*Tg*), melting temperature (*Tm*), and crystallization temperature (*Tc*). Measurements were conducted using a Perkin-Elmer DSC 8500 device. For sample preparation, approximately 5−8 mg of dry solid sample was weighed directly into an aluminum pan to minimize sample loss. The pan was sealed with a lid, positioned with its indented side facing downward, using a Perkin-Elmer universal crimping press. A second empty aluminum pan, prepared under identical conditions, was used as a reference.

https://doi.org/10.1021/acssuschemeng.5c03946
ACS Sustainable Chem. Eng. XXXX, XXX, XXX−XXX

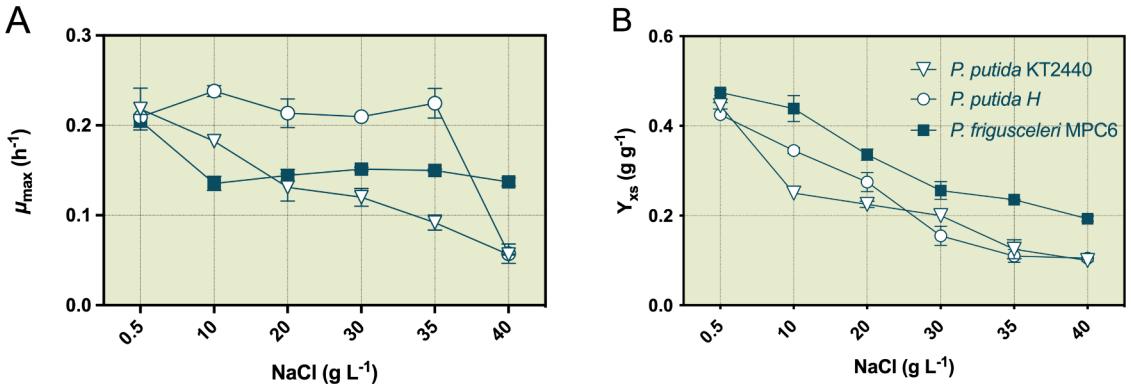

Figure 1. Growth behavior and biomass formation of various *Pseudomonas* strains under different salt concentrations. (A) Specific growth rate and (B) biomass yields of *P. putida* KT2440, *P. putida* H, and *P. frigusceleri* MPC6 cultivated on 4 g L^{-1} glycerol in shake flask experiments. Values represent the mean and standard deviation from three independent biological replicates.

The DSC analysis was carried out under a nitrogen purge gas flow maintained at 30 cm^3 min-1 and a system pressure of 20 psi. Pyris DSC software was utilized to control the instrument and manage data acquisition. The thermal protocol included: cooling from 30.00 °C to −20.00 °C at a rate of 20.00 °C/min, holding at −20.00 °C for 5 min, heating from −20.00 to 200.00 °C at the same rate, holding at 200.00 °C for 2 min, cooling back to −20.00 °C at 20.00 °C min^{-1}, holding at −20.00 °C for 5 min, and finally reheating to 200.00 °C at 20.00 °C min^{-1}. Before analyzing the samples, a baseline was recorded using empty pans, which was subtracted from the sample data to eliminate background signals. The first heating step was employed to remove the sample's thermal history, while the subsequent cooling and reheating cycles were used to determine key thermal properties, such as *Tg, Tm, Tc*, crystallinity (J g^{-1}), and heat capacity (J g^{-1} $°C^{1-}$). Final results were saved as PDF files or exported in text format for further analysis.

2.10. GPC Analysis. The molecular weight and molecular weight distribution of the polymer samples were determined using an Agilent 1260 Infinity II Gel Permeation Chromatography (GPC) system (Agilent Technologies, UK) equipped with a Dual Angle Light Scattering Detector (LS), a Refractive Index Detector (RI), and a Viscometer. The mobile phase was HPLC-grade chloroform, used isocratically at a flow rate of 1 mL min^{-1} and a column temperature of 50 °C. Detector temperatures were maintained at 40 °C. For sample preparation, approximately 1−2 mg of purified polymer was dissolved in chloroform to prepare solutions with concentrations adjusted according to polymer size: ∼ 2 mg mL^{-1} for smaller polymers and ∼ 1 mg mL^{-1} for larger polymers. Dissolution was performed without vortexing or sonication, allowing natural dissolution at room temperature for a minimum of 1 h, preferably overnight. The solutions were then filtered through a 0.1−0.2 μm hydrophobic PTFE membrane to remove particulates. Column calibration was performed using polystyrene standards from the Poly(styrene) Medium Low Kit (Mp 162−851,000 Da, PSS Polymer Standards Service GmbH, Germany), with a nominal Mp calibration point of 131,700 g mol^{-1}. The calibration ensured consistent instrument performance and was used as a reference for molecular weight determination. Each sample was analyzed with an injection volume of 100 μL and a run time of 36 min.

2.11. Nuclear Magnetic Resonance (NMR) Spectroscopy. The purity and structure of the polymer were evaluated using nuclear magnetic resonance (NMR) spectroscopy. One-dimensional proton (1H) NMR experiments were performed for each sample on a Bruker AV III 600 MHz spectrometer equipped with a 24-sample cooled loader (Sample Case Standard). Approximately 4 mg of the extracted polymer was dissolved in 200 μL of deuterated chloroform ($CDCl_3$) and transferred to a 5 mm NMR tube. After ensuring complete dissolution, the tube was sealed and loaded into the magnet. All experiments were conducted at 298 K (25 °C). For the ^{1}H NMR analysis, the parameters included a spectral width of 12 ppm, a time domain of 32,768 points, and 16 scans per sample. The ^{13}C-spectra were acquired with the default pulse sequence zgpg30 (power-gated 30 ° pulse) with a spectral width of 309 ppm, 20480 points, 6400 scans, and 6.5 s relaxation delay. The HSQC spectra were acquired with a spectral width of 10 ppm and 200 ppm for proton and ^{13}C, respectively. The spectra were obtained in standard acquisition mode with 2048 points for proton and 128 points for carbon. Data were processed and analyzed using TopSpin 4.1 (Bruker Biospin, Rheinstetten, Germany) and MestreNova v15.1.0 software. Chemical shifts are reported in ppm, with tetramethylsilane (TMS) as the internal standard.

2.12. 16S rRNA Gene Amplicon Sequencing and Analysis. The composition of the bacterial community was analyzed using 16S rRNA gene amplicon sequencing. Aliquots of 10 mL were centrifuged at 9,000 × g and 4 °C for 10 min. The supernatant was discarded, and the pellet was washed three times with 0.9% (w v^{-1}) NaCl. Genomic DNA was extracted using the GeneJET DNA Purification Kit (Thermo Fisher Scientific, Waltham, MA, USA). DNA integrity and concentration were evaluated by 1% agarose gel electrophoresis and by measuring the OD 260/280 ratio. The DNA samples were subsequently sent to the Dalhousie University Integrated Microbiome Resource (IMR; imr.bio) for 16S rRNA amplicon sequencing of the V4−V5 region. Amplicons were generated using modified primers as described elsewhere[28] and following the protocol described by Comeau et al.[29] Sequencing was performed using 300 + 300-bp paired-end (PE) v3 chemistry on an Illumina MiSeq platform.

Sequence data were processed using amplicon sequence variants (ASVs) with DADA2 v1.8.[30] The filtering parameters for 16S rRNA gene sequences were set as follows: maxN = 0, maxEE = c(2,2), and truncQ = 2, with trimming parameters at truncLen = c(220,150). Error rate learning, dereplication, denoising, and merging were conducted according to the DADA2 Pipeline Tutorial (v1.16).

2.13. Strain Confirmation by 16S rRNA Amplicon (Sanger) Sequencing. At the end of the fermentation, 1 mL of culture was serially diluted in sterile phosphate-buffered saline (PBS) and spread onto LB agar plates supplemented with 25 g L^{-1} NaCl. After 24 h of incubation at 30 °C, four colonies were randomly picked, and genomic DNA was extracted using the GeneJET Genomic DNA Purification Kit (Thermo Fisher Scientific). The 16S rRNA gene was PCR-amplified, and amplicons were Sanger sequenced (Macrogen, USA) with universal primers 27F(5′-AGAGTTTGATCCTGGCT-CAG-3′) and 1492R (5′-TACGGYTACCTTGTTACGACTT-3′). Resulting sequences were compared against reference databases using BLASTn on the NCBI Web site.

2.14. Statistical Analysis. All shake flask experiments were performed in triplicate, and the results are presented as mean values with error bars representing the standard deviation of the replicates. Bioreactor experiments were conducted in triplicates. Statistical analysis was performed using GraphPad Prism 5.0 (GraphPad Software, Inc., San Diego, CA, USA). Group comparisons were

https://doi.org/10.1021/acssuschemeng.5c03946
ACS Sustainable Chem. Eng. XXXX, XXX, XXX−XXX

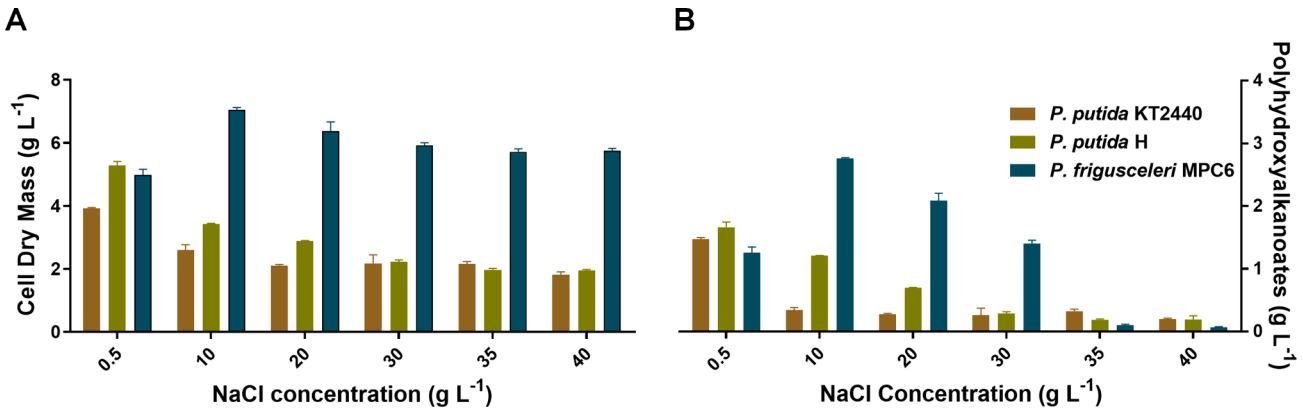

Figure 2. Total biomass and PHA production of various *Pseudomonas* strains under different salt concentrations after 72 h of cultivation. (A) Total biomass and (B) PHA concentrations of *P. putida* KT2440, *P. putida* H, and *P. frigusceleri* MPC6 cultivated on 30 g L^{-1} glycerol in shake flask experiments. Values represent the mean and standard deviation from three independent biological replicates.

made using one-way analysis of variance (ANOVA), with differences considered statistically significant at a *p*value of < 0.05.

3. RESULTS AND DISCUSSION

3.1. Inhibitory Effect of Sodium Chloride on Growth Rates and Biomass Yields of Different *Pseudomonas* Strains. We first evaluated the impact of increasing salt concentrations on important cell physiological parameters such as the maximum specific growth rate (μ_{max}) and biomass yield of well-reported PHA producers, including *Pseudomonas putida* KT2440[15], *P. putida* H[6], and *P. frigusceleri* MPC6 growing with 4 g L^{-1} glycerol in axenic shake-flask cultivations. Remarkably, *P. putida* H maintained a specific growth rate of 0.19 h^{-1} despite the upshift on the salt concentration—from 0.5 to 35 g L^{-1} (Figure 1A). The model strain *P. putida* KT2440 was more sensitive to the imposed osmotic conditions showing a negative correlation between μ_{max} and the salt concentration in the growth medium. However, the Antarctic *P. frigusceleri* MPC6 retained a growth rate of 0.13 h^{-1} even in the presence of 40 g L^{-1} NaCl while the growth rate of *P. putida* KT2440 and H showed a 4-fold decrease (Figure 1A). In addition, increasing salt concentrations significantly reduced biomass yield coefficients for all tested *Pseudomonas* strains, being the MPC6 cells with the highest yield recorded under high osmolarity (Figure 1B). In this context, environmental bacteria commonly adjust the intracellular osmotic state by expending energy, in the form of ATP, and overexpressing membrane proteins and osmoprotectant metabolites.[31] This energetic process results in heat dissipation which can activate key metabolic reactions enabling cell propagation at a high rate at the expense of biomass formation.[32] This rate-yield tradeoff is crucial when selecting an appropriate PHA producer under osmotic stress as low growth rates particularly impact the specific volumetric productivity or reduced biomass results in less PHA titers as the biopolymer accumulates intracellularly.

3.2. PHA Synthesis with Different NaCl Amounts in Batch Cultures. To evaluate PHA and biomass formation in batch cultures, we increased the glycerol concentration from 4 to 30 g L^{-1} to trigger nitrogen limitation and quantify biopolymer yields after 72 h of cultivation. NaCl concentrations ranging from 10 to 40 g L^{-1} caused a reduction in the cell dry weight (total biomass) and PHA by nearly 50% and 80%, respectively, in *P. putida* KT2440 (Figure 2). *P. putida* H endured the salt upshifts, from 0.5 to 10 g L^{-1}, while the CDW and PHA declined from 5.28 and 1.66 g L^{-1} to 3.43 and 1.20 g L^{-1}, respectively. For the rest of the experiments, there was a considerable decrease in biomass (~60%) and cells accumulated nearly 0.2 gPHA L^{-1}. Notably, *P. frigusceleri* MPC6 showed a different trend from the other *P. putida* strains as the bacterium produced more biomass and biopolymers in experiments supplied with 20 and 10 g L^{-1} NaCl (Figure 2), with the latter salt concentration showing the best PHA titer (2.76 g L^{-1}, 98% increase). *P. frigusceleri* cells producing PHA (1.4 g L^{-1}) in broth cultures containing 30 g L^{-1} of NaCl were similar to that obtained at 0.5 g NaCl L^{-1} (control) and declined more than 90% for the other experiments (Figure 2).

Augmented salt levels have been shown to be beneficial for PHB synthesis in the industrial biopolymer producer *C. necator*, which accumulated 30% more PHB when grown with 9 g NaCl L^{-1} on acetate.[33] As reported here, moderate salt concentrations can inhibit *mcl*-PHA as shown by other microorganisms producing PHB synthesis.[33,34] In another study, *Vibrio proteolyticus* retained the accumulated PHB at more than 50% of the cell mass when cultivated in up to 50 g L^{-1} of NaCl.[35] Beyond this concentration, PHB and biomass production declined under nonsterile conditions. It is clear that the capacity to accumulate PHAs in halotolerant microorganisms is dependent on the niche from which they were isolated.[36] Based on our results none of the *P. putida* strains displayed better PHA production performance under hypertonic conditions except for the Antarctic *P. frigusceleri* MPC6. We showed recently that this bacterium propagates at a high rate at low temperature (4 °C) and synthesized similar biomass and PHA amounts to those obtained in bioreactors run at 30 °C.[20] Psychrotolerant bacteria share many molecular systems to encounter osmotic stress and cold environments like proline, trehalose, and polysaccharide overproduction, a boost in protein levels involved in maintaining membrane fluidity, fighting oxidative stress, and assuring DNA replication, translation, and cofactor synthesis.[31] As the MPC6 strain was isolated from the Antarctic Deception Island,[20] it might also confront fluctuations in salt concentrations in addition to temperature. We recently reported that this bacterium can intracellularly bioreduce selenite into selenium nanoparticles while propagating in natural seawater supplemented with crude glycerol.[22] Analysis of the genome of MPC6 reveals that it harbors more than 20 glutathione-related proteins, trehalose synthesis and transport, and stabilizing DNA proteins.[21] These molecular traits might partly support good growth at both cold temperatures and high osmolarity.[10]

https://doi.org/10.1021/acssuschemeng.5c03946
ACS Sustainable Chem. Eng. XXXX, XXX, XXX−XXX

Table 1. Monomer Composition of the Biosynthesized PHA by *P. putida* KT2440, *P. putida* H and *P. Frigusceleri* MPC6 Grown on Glycerol (30 G L^{-1}) in Shake Flask Experiments After 72 h of Cultivation[c]

	NaCl	monomer composition (%)[b]						
strain	(g L^{-1})	3HB	3HH	3HO	3HD	3HC12:1	3HDD	3HT
P. putida	0.5	ND.[a]	3.7	20.7	72.1	1.2	2.3	0.9
KT2440	5	ND.	3.3	24.1	64.3	4.7	3.6	ND.
	10	ND.	4.1	24.6	63.4	4.8	3.1	ND.
	20	ND.	4.2	28.8	59.8	4.7	2.5	ND.
	30	ND.	4.5	27.7	60.3	4.6	2.9	ND.
	35	ND.	4.3	27.3	60.8	4.4	3.2	ND.
	40	ND.	4.4	24.7	63.3	5.1	2.5	ND.
P. putida H	0.5	ND.	4	27.9	62.2	0.3	5.6	ND.
	5	ND.	3.4	24.1	64.2	3.6	4.7	ND.
	10	ND.	3.7	25	64.1	4.4	2.8	ND.
	20	ND.	4.8	23.5	61.2	5.7	4.8	ND.
	30	ND.	4.7	24	61.3	6.0	4.0	ND.
	35	ND.	3.5	25.1	61.7	5.7	4.0	ND.
	40	ND.	5.4	23.5	62.3	5.8	3.8	ND.
P. frigusceleri	0.5	89.4	1.8	3.3	4.4	ND.	1.1	ND.
MPC6	5	87.3	1.3	4.1	5.5	ND.	1.8	ND.
	10	86.1	1.5	4.6	6.9	ND.	0.9	ND.
	20	85.7	1.6	4.2	6.8	ND.	1.7	ND.
	30	86.5	1.8	3.9	6.5	ND.	1.3	ND.
	35	86.3	1.7	4.7	6.3	ND.	1.0	ND.
	40	86.8	1.3	5.1	5.9	ND.	0.9	ND.

[a]ND. Not detected. [b]3HB: 3-hydroxybutyrate, 3HH: 3-hydroxyhexanoate, 3HO: 3-hydroxyoctanoate, 3HD: 3-hydroxydecanoate, 3HDD: 3-hydroxydodecanoate, 3HC12:1: 3-hydroxy-5-cis-dodecanoate, 3HT: 3-hydroxytetradecanoate. [c]Data reflect mean values from three replicates.

We also analyzed the monomer composition of the biosynthesized PHA by the *Pseudomonas* strains via GC-MS (Table 1). *P. putida* KT2440 and H synthesized the distinctive *mcl*-PHA with 3-hydroxydecanoate (3HD) as the major monomer of the polyester under standard growth conditions. Salt upshifts resulted in an enrichment of unsaturated monomers (3HC12:1), increasing from 1% to ∼ 6% of the relative polymeric content along with the absence of 3-hydroxydodecanoate (3HT) in the formed mcl-PHA for both *P. putida* strains. On the other hand, glycerol-grown MPC6 cells produced *short*- and *medium*-chain length PHAs having 3-hydroxybutyrate (C4, > 85%) as the dominant monomer, followed by 3-hydroxydecanoate (C10, > 5%). Besides, high osmolarity has no significant effect in the monomer composition of the synthesized PHA by *P. frigusceleri* MPC6, presenting only saturated monomers within the polymeric chain (Table 1).

3.3. Kinetics of PHA Production on Pure and Crude Glycerol in Nonsterile Batch Bioreactors. We next evaluated growth and PHA formation kinetics of *P. frigusceleri* MPC6 with 20 g L^{-1} NaCl and 30 g L^{-1} of pure and crude glycerol for comparison in batch bioreactors. Although this salt content promotes an enhanced PHA synthesis in shake-flask experiments (Figure 2), it did not prevent contamination in the fermenter (data not shown). We therefore increased the salt content to 25 g L^{-1}. In this setting using pure glycerol, *P. frigusceleri* depleted the available ammonium within the first 24 h, reaching a CDW of 3 g L^{-1} and accumulating some amount of PHA within the cell (Figure 3B). At 72 h of cultivation, glycerol remained within the culture broth and PHA represented 42% of the CDW. Conversely, under axenic conditions, glycerol was completely consumed after 72 h (Figure 3A), and *P. frigusceleri* produced similar PHA titers to those observed in the nonsterile bioreactors (Figure 3A, B). Within axenic bioreactors fed with crude glycerol, CDW was the highest among the tested conditions, achieving 6.5 g L^{-1} at the end of the process (Figure 4A). The produced PHA did not significantly vary compared to the use of pure glycerol (Figure 4A, 3A). Further, salt-supplemented batch bioreactors running with crude glycerol also produced 0.03 g L^{-1} h^{-1} PHA and formed 5.5 g L^{-1} of CDW (Figure 4B), which represents 15% less CDW compared to sterile bioreactors (Figure 4A, B).

To investigate the presence of other bacteria growing with *P. frigusceleri* in open batch bioreactors, we used 16S rRNA amplicon sequencing to determine microbial composition on samples taken at the end of the fermentation period. *P. frigusceleri* represented more than 92% and 98% of the bacterial abundance for cells grown with pure and crude glycerol at the genus level, respectively (Figure 3B, 4A). In pure glycerol, bacteria belonging to the genera *Candida* (4.2%), *Paracoccus* (0.6%), and *Nitrosomonas* (0.3%) propagated together with *Pseudomonas* (Figure 3B).

However, in nonsterile batch bioreactors converting crude glycerol to PHA, *Klebsiella* (1.6%) was the only bacterium growing along with *Pseudomonas* (Figure 4A). These results confirm that using NaCl favored the prevalence of strain MPC6 when producing PHA on glycerol, with industrial crude glycerol imposing a more restrictive environment. Although *P. frigusceleri* MPC6 is phylogenetically distinct from typical mesophilic *Pseudomonas* strains prevalent in the American continent,[37] ∼ 300 bp 16S rRNA amplicon reads are too short to resolve *Pseudomonas* at the species level. Thus, we obtained CFU counts at the end of the PHA production process on LB plates supplemented with 25 g L^{-1} NaCl to visualize colony

https://doi.org/10.1021/acssuschemeng.5c03946
ACS Sustainable Chem. Eng. XXXX, XXX, XXX−XXX

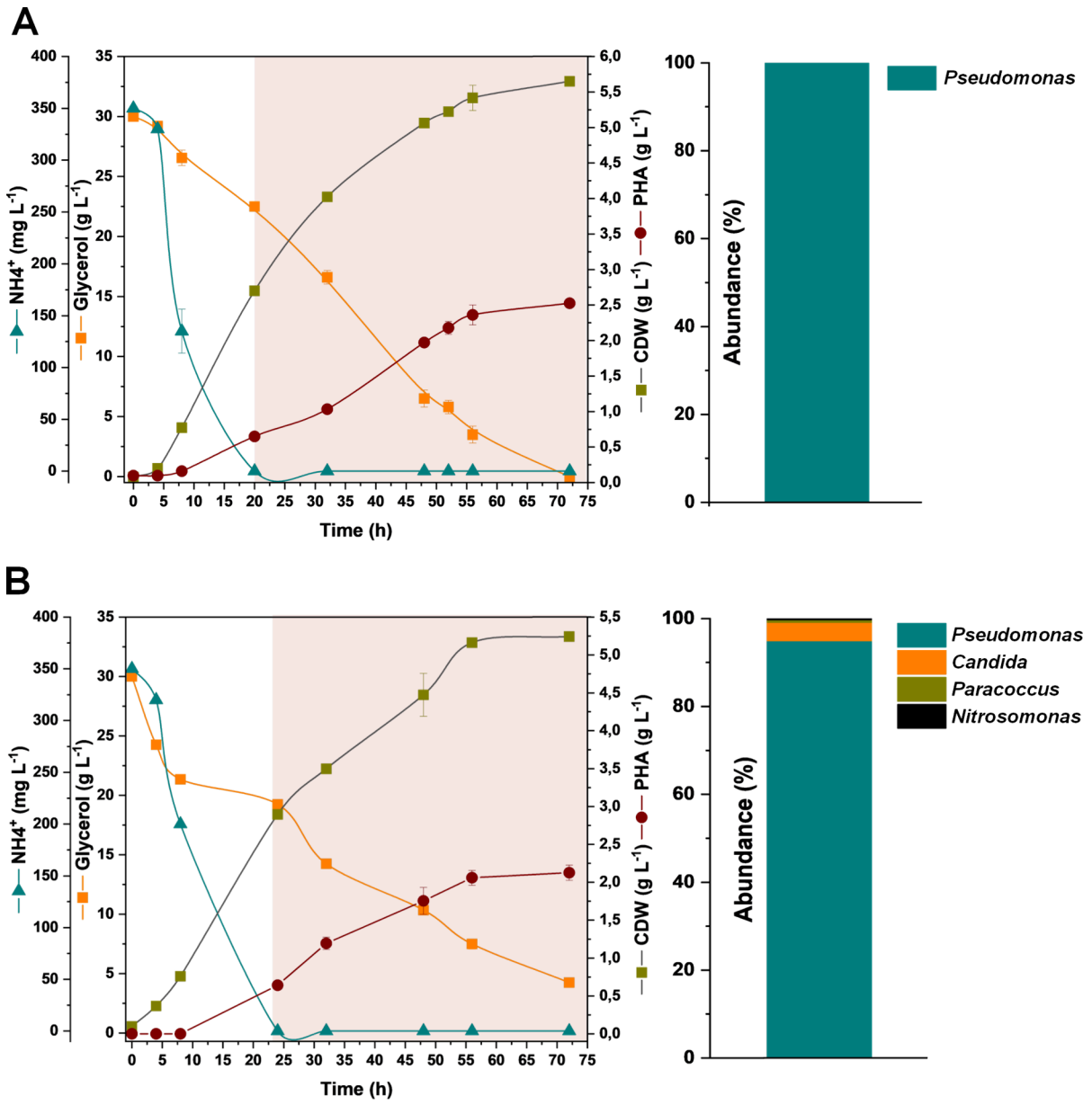

Figure 3. Time course of glycerol and ammonium consumption, total biomass formation, and PHA production by *P. frigusceleri* MPC6. 16S rRNA amplicon sequencing analysis was conducted at 72 h of cultivation. (A) axenic bioreactor containing 30 g L^{-1} pure glycerol and no salt addition and (B) open batch bioreactor containing 30 g L^{-1} pure glycerol and 25 g L^{-1} NaCl. Values represent the mean and standard deviation from three independent bioreactor experiments.

morphology. The CFU values were 4.1−5.6 × 10^{11} CFU mL^{-1}. In the serial dilutions used for counting, we observed only *P. frigusceleri*-like colonies, which showed mucoid, spreading growth (Supporting Information). Sanger sequencing of 16S rRNA genes from representative colonies using universal primers showed > 99.6% identity to *P. frigusceleri* MPC6 (Supporting Information). This indicates that higher-resolution, long-read sequencing (e.g., Nanopore or PacBio) is needed to resolve *Pseudomonas* to the species level in mixed cultures. Taken together, we confirmed that *P. frigusceleri* was responsible for PHA biosynthesis in nonsterile batch bioreactors. Biodiesel-derived crude glycerol exerts a toxic effect on many bacteria as it contains ashes, metals, and methanol.[8] It appears that bacteria growing together with *P. frigusceleri* in pure glycerol are more sensitive to compounds comprising crude glycerol as they were not present in the open batch bioreactor (Figure 4A). Besides, *Klebsiella* strains are robust bacterial workhorses capable of converting crude glycerol into 1,3-propanediol and 3-hydroxypropionate and a suitable bacterium to emerge in this environment spontaneously.[38,39] More importantly, the recorded abundance of *Klebsiella* spp. was low (1.6%) in the fermenter, which did not affect the total PHA yield (Table 2).

To capture possible morphological changes in *P. frigusceleri* cells grown with different kinds of glycerol and high osmolarity, we sampled the bioreactors when PHA formed at the maximum level and fixed the cells further to carry out transmission electron microscopy (TEM). *P. frigusceleri* MPC6 exhibited a thick membrane and accumulated irregular PHA granules for both conditions (Figure 5A, B). The cells were significantly smaller (p-value < 0.05) in open batch bioreactors containing pure glycerol compared to crude glycerol (Figure

https://doi.org/10.1021/acssuschemeng.5c03946
ACS Sustainable Chem. Eng. XXXX, XXX, XXX−XXX

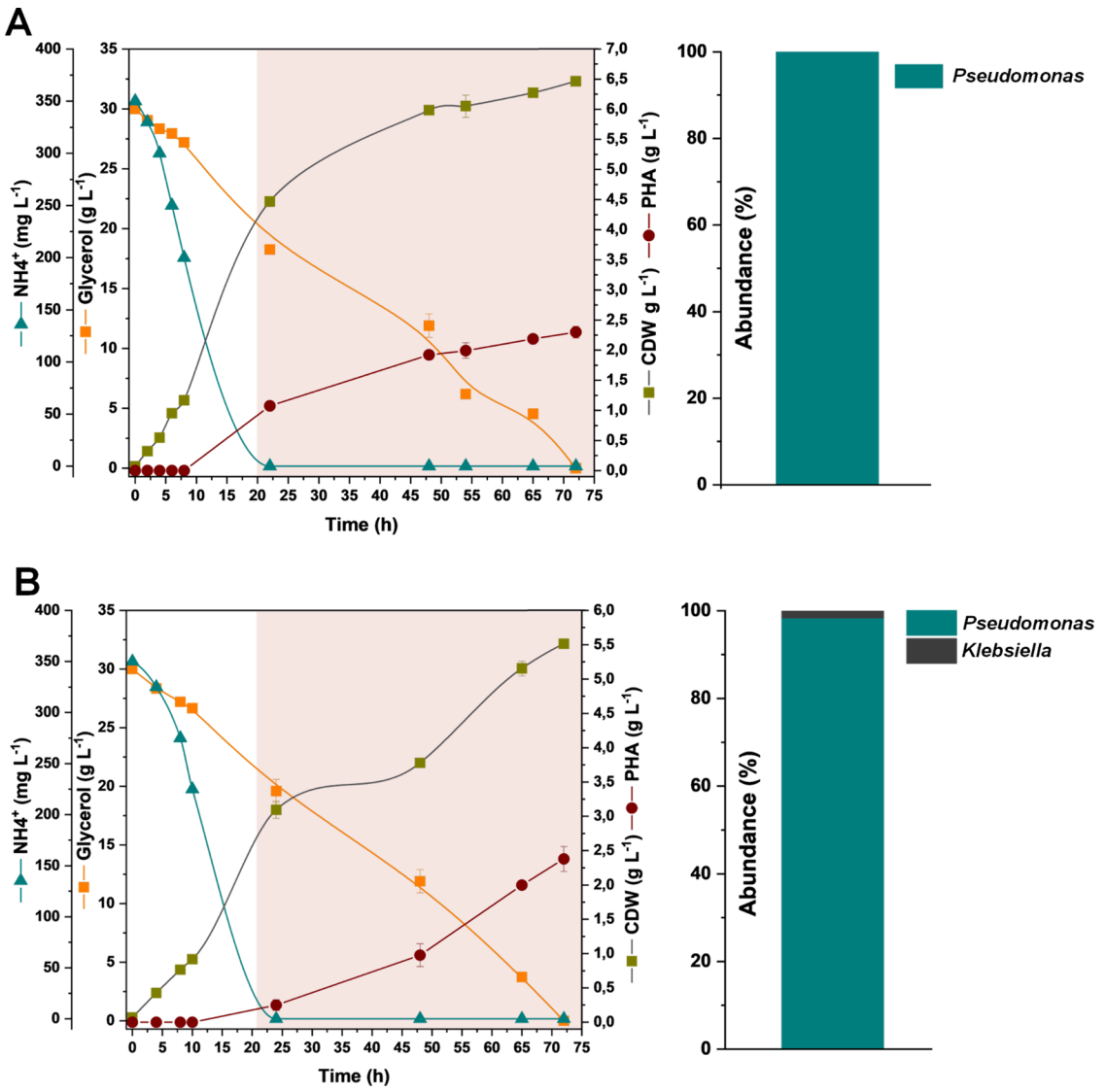

Figure 4. Time course of glycerol and ammonium consumption, total biomass formation, and PHA production by *P. frigusceleri* MPC6. 16S rRNA amplicon sequencing analysis was conducted at 72 h of cultivation. (A) axenic bioreactor containing 30 g L^{-1} crude glycerol and no salt addition and (B) open batch bioreactor containing 30 g L^{-1} crude glycerol and 25 g L^{-1} NaCl. Values represent the mean and standard deviation from three independent bioreactor experiments.

5C). The same phenomenon has been previously reported for MPC6 cells producing PHA at 4 °C[20]. Certain bacteria can reduce their cell body size to retain the protein synthesis rate, which in turn maintains growth rates under adverse conditions.[40] Besides temperature, osmolarity appears to be another factor that brings about the formation of smaller MPC6 cells.[41] Moreover, given the prominent cell membrane thickness visualized in the micrographs, we characterized the lipid membrane composition of *P. frigusceleri* as the alteration of fatty acids is a widespread survival mechanism in bacteria to retain membrane homeostasis and fluidity.[42,43] Whereas the primary membrane fatty acids were C16 and C16:11, increased NaCl had no significant impact on the types and proportions of fatty acids comprising the cell membrane of *P. frigusceleri* (Table 2). Besides the modulation of the ratio of *trans* to *cis* unsaturated fatty acids,[44] psychrotolerant *Pseudomonas* strains also increase the cyclic fatty acids content by activating a cyclopropane phospholipid synthase enzyme (Cfa) at low temperature,[45] whereas the total saturated fatty acid content, particularly the C17:0 cyclopropane fraction, increased when *P. putida* mt-2 was challenged with hypertonic conditions in planktonic cultures.[46]

3.4. Thermal properties, Mw, and PDI of PHA Produced in Batch Bioreactors. Differential scanning calorimetry measurements were obtained to decipher key thermal features of the biosynthesized PHAs. We observed differences between melting temperature (*Tm*), but not for glass (*Tg*), and transition (*Tc*) temperatures of biopolymers derived from pure and crude glycerol (Table 3). The addition of NaCl to *P. frigusceleri* bioreactors growing on pure glycerol decreased the melting temperature of the produced PHA compared to the control, while the use of crude glycerol enhanced the *Tm* values toward 179 °C. The average-molecular weights (*Mw*) of purified PHAs derived from crude glycerol, regardless of the presence of NaCl, were in the range of 460−640 kDa, which are relatively similar to the PHA produced on pure glycerol (490 kDa, Table 3). This was not the case for the polyester biosynthesized under hypertonic

https://doi.org/10.1021/acssuschemeng.5c03946
ACS Sustainable Chem. Eng. XXXX, XXX, XXX−XXX

Table 2. Cellular Membrane and Monomer Composition of the Biosynthesized PHA in *P. frigusceleri* MPC6 Cultured on 30 g L^{-1} Glycerol in Bioreactors After 72 h [NaCl Concentration 25 (g L^{-1})]

condition	CDW	PHA	monomer composition (%)[c]					
	(g L^{-1})	(g L^{-1})	3HB	3HH	3HO	3HD	3HDD	3HC12:1
glycerol	5.48 ± 0.2[a]	2.60 ± 0.1	89.5 ± 1.2	1.8 ± 0.1	3.3 ± 0.1	4.4 ± 0.3	1.1 ± 0.0	ND.[b]
glycerol (NaCl)	5.34 ± 0.2	2.05 ± 0.1	87.1 ± 3.3	1.7 ± 0.1	5.2 ± 0.7	4.3 ± 0.1	1.7 ± 0.1	ND.
crude glycerol	6.23 ± 0.1	2.19 ± 0.1	84.1 ± 2.1	1.6 ± 0.2	6.5 ± 0.1	5.7 ± 0.4	2.1 ± 0.2	ND.
crude glycerol (NaCl)	5.76 ± 0.3	2.41 ± 0.2	83.7 ± 5.0	1.3 ± 0.1	6.2 ± 0.9	5.3 ± 0.1	3.6 ± 0.3	ND.

condition	membrane composition (%)[d]					
	C12	C14	C16:11	C16	C17:10	C18:11
glycerol	7.3 ± 0.2	2.9 ± 0.0	26.7 ± 2.7	42.6 ± 0.4	13.8 ± 0.1	12.1 ± 0.2
glycerol (NaCl)	5.3 ± 0.1	2.5 ± 0.0	23.6 ± 0.5	46.1 ± 0.7	13.5 ± 0.2	5.9 ± 0.2
crude glycerol	5.8 ± 0.1	1.8 ± 0.0	25.5 ± 0.2	43.1 ± 0.5	11.1 ± 0.2	9.2 ± 0.2
crude glycerol (NaCl)	5.7 ± 0.2	2.1 ± 0.0	27.7 ± 0.1	46.6 ± 0.8	8.3 ± 0.1	6.9 ± 0.1

[a]The data reflect mean values and deviation from three independent bioreactors. [b]ND. Not detected [c]3HB: 3-hydroxybutyrate, 3HH: 3-hydroxyhexanoate, 3HO: 3-hydroxyoctanoate, 3HD: 3-hydroxydecanoate, 3HDD: 3-hydroxydodecanoate, 3HC12:1: 3-hydroxy-5-cis-dodecanoate, 3HT: 3-hydroxytetradecanoate. [d]C12; dodecanoic acid, C14; tetradecanoic acid, C16:11; 11-cis palmitic acid, C16; palmitic acid, C17:10; 10 cis-heptadecanoic acid; C18:11; 11 cis-stearic acid.

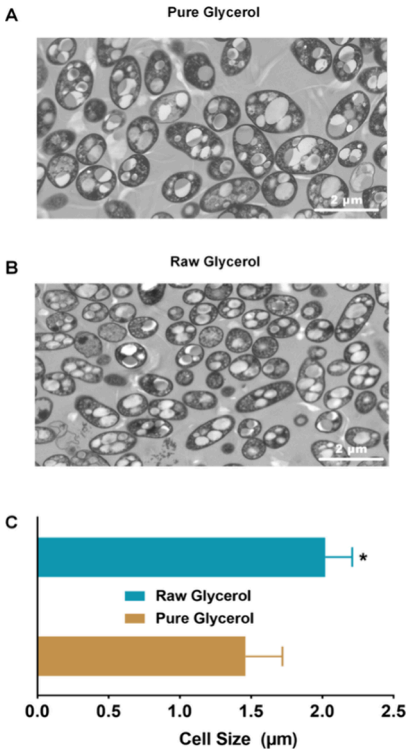

Figure 5. Transmission electron microscopy (TEM) of *P. frigusceleri* cells producing PHA in unsterile open batch bioreactors after 72 h of cultivation. (A) TEM micrographs of cells cultured on pure glycerol, (B) TEM micrographs of cells cultured on raw glycerol, and (C) cell size distribution of *P. frigusceleri* MPC6; *p value < 0.05 indicates statistical significance.

conditions with pure glycerol, as its *Mw* was significantly higher (almost two times) compared to the PHA obtained with salt addition (Table 3.) More importantly, the PDI values were significantly reduced when raw glycerol and the addition of NaCl were employed for biopolymer production in bioreactors, displaying PDI values from 1.6 to 2.4. These results indicate that the use of crude glycerol alongside the addition of NaCl led to narrow weight distributions of purified PHAs, an important feature for thermoforming and industrial extrusion of polymers. The incorporation of monomers other than 3HB, at more than 20 mol% as blends or copolymers in the resulting PHAs has been widely reported to increase PDI values.[47−49] The ratio M_w/M_n of PHAs is governed by several factors, with the activities of the PhaC synthase enzyme during the polymerization process and the counteraction of the PhaZ depolymerase reported as key players.[48,50]

3.5. PHA Fed-Batch Production and Biopolymer Properties in Unsterile Bioreactors. We then conducted a fed-batch process using crude glycerol as the only C-substrate during the entire process. The system had three stages: i) a batch phase, ii) an exponential phase for biomass formation, and iii) a nitrogen limiting phase where crude glycerol was fed to the bioreactor pulse-wise (DO-stat) for PHA production. Within the batch phase, biomass reached ∼ 9 g L^{-1} after 18 h (Figure 6A). Then, the exponential feeding of glycerol began, during which compressed air was enriched with pure oxygen (1:10, O_2:air) to avoid oxygen limitation as stirring the bioreactor at 1,200 rpm could not maintain the DO value above 20% when only air was supplied. Glycerol was completely metabolized throughout this stage and after 26 h of cultivation, the culture reached 30 g L^{-1} of total biomass; no PHA was observed because ammonium was still present within the culture broth (Figure 6A).

At this point, we stopped the addition of external ammonium and fed crude glycerol following a DO response by providing pulses. This approach led to a nitrogen limiting regime while *P. frigusceleri* began to synthesize PHA. During the DO-stat feeding strategy (phase iii) and nitrogen limitation, the pure-oxygen supply was discontinued and only compressed air was provided to the fed-batch bioreactor to obtain a better and faster DO response of the culture's oxygen demand.[51] PHA boosted within the cells between 26 and 46 h. The PHA titer peaked at 46 h (21.4 gPHA L^{-1}), and this concentration was maintained until the end of the process despite feeding more crude glycerol to the bioreactor (Figure 6A). No metabolic byproducts like acetic acid were detected (data not shown). Overall, *P. frigusceleri* had a total PHA yield on glycerol of 0.19 gPHA $gGly^{-1}$ and a specific PHA volumetric productivity of 0.47 g L^{-1} h^{-1} under nonsterile conditions. We also examined the proportion of micro-

https://doi.org/10.1021/acssuschemeng.5c03946
ACS Sustainable Chem. Eng. XXXX, XXX, XXX−XXX

Table 3. Monomer Composition, Average Molecular Weights, Polydispersity Index, and Thermal Properties of PHA Produced from Glycerol by *P. frigusceleri* MPC6 under Different Fermentation Conditions and Salt Concentrations[a]

condition	fermentation mode	T_m (°C)[θ]	T_g (°C)	T_c (°C)	*Mw* (kDa)	*Mn* (kDa)	PDI	reference
glycerol	batch	163.5	2.3	45.9	490	118	4.1	20
glycerol (NaCl)*	batch	150.3 ± 1.1	1.9 ± 0.1	55.3 ± 0.1	965	603	1.6	this study
crude glycerol	batch	179.2 ± 0.4	2.7 ± 0.3	56.1 ± 0.3	462	193	2.4	this study
crude glycerol (NaCl)	batch	176.5 ± 0.2	2.9 ± 0.3	52.0 ± 0.4	515	245	2.1	this study
crude glycerol (NaCl)	fed-batch (46 h)	174.7 ± 0.3	3.1 ± 0.4	55.7 ± 0.3	633	330	1.9	this study
crude glycerol (NaCl)	fed-batch (52 h)	173.3 ± 0.4	3.5 ± 0.2	57.9 ± 0.5	348	175	2.0	this study
		3HB	3HH	3HO	3HD	3HDD	3HC12:1	
crude glycerol (NaCl)	fed-batch (46 h)	87.1 ± 0.5	0.3 ± 0.0	5.4 ± 0.1	7.2 ± 0.3	ND.	ND.	this study
crude glycerol (NaCl)	fed-batch (52 h)	88.3 ± 0.3	0.7 ± 0.1	4.1 ± 0.2	6.9 ± 0.1	ND.	ND.	this study

[a]Values represent the mean and standard deviation from three independent bioreactor experiments. *NaCl (25 g L^{-1}). T_m, melting temperature; T_g, glass transition temperature; T_c, crystallization phase transition temperature; *Mw*, average molecular weight; *Mn*, molecular mass distribution; and PDI, polydispersity index. ND. Not detected. 3HB: 3-hydroxybutyrate, 3HH: 3-hydroxyhexanoate, 3HO: 3-hydroxyoctanoate, 3HD: 3-hydroxydecanoate, 3HDD: 3-hydroxydodecanoate, 3HC12:1: 3-hydroxy-5-cis-dodecanoate, 3HT: 3-hydroxytetradecanoate. [θ]T_m, T_g, and T_c values were obtained from the second heating curves of the DSC analysis.

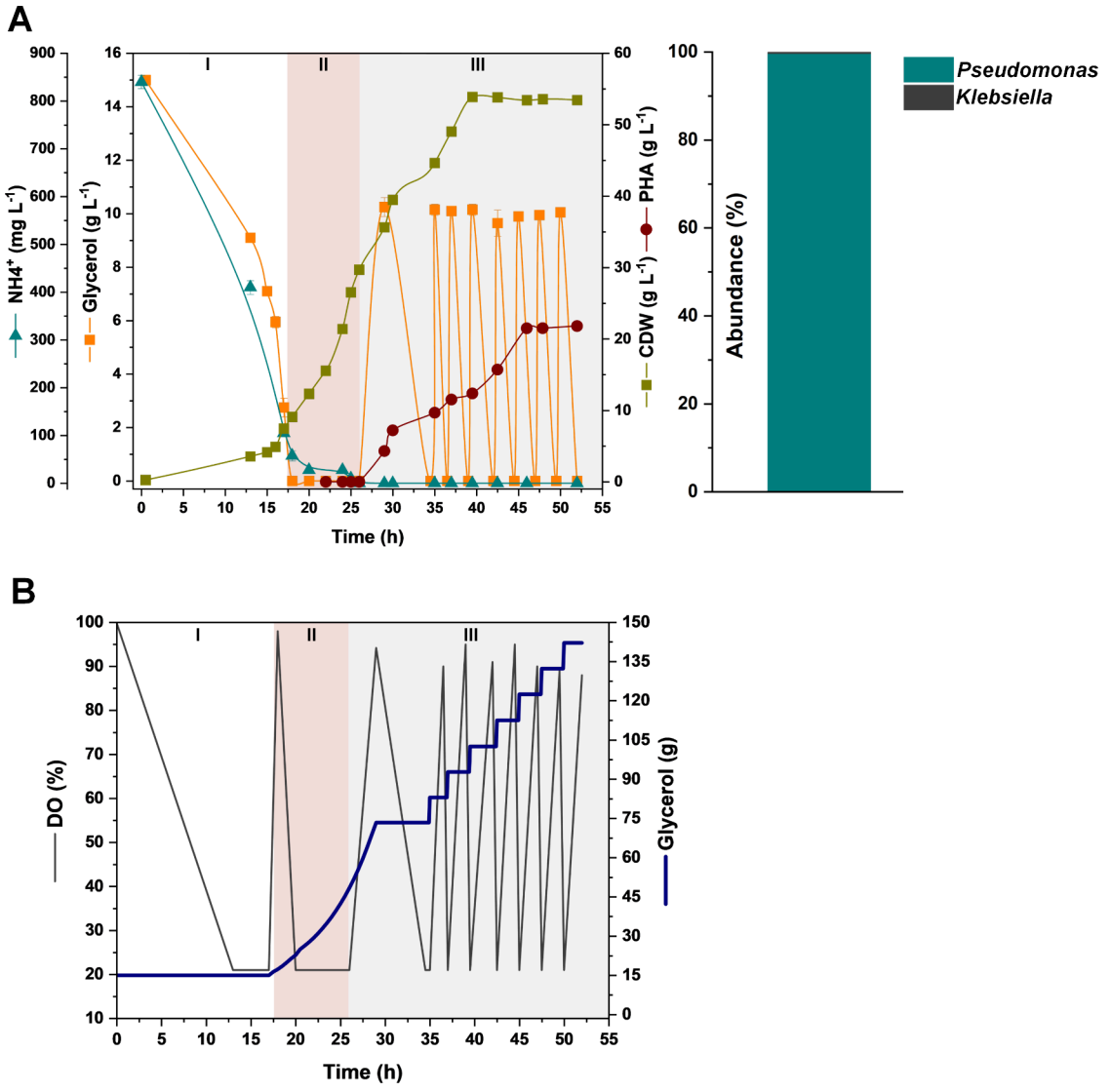

Figure 6. Open fed-batch PHA production using *P. frigusceleri* cultured on crude glycerol as the sole carbon substrate and 25 g L^{-1}NaCl. The fermentation process consisted of multiple feeding stages: (I) batch culture, initial crude glycerol concentration of 15 g L^{-1}, (II) exponential feeding (μ_{set} = 0.12 h^{-1}), and (III) DO-stat crude glycerol feeding. (A) Substrate and product profiles of *P. frigusceleri* and 16S rRNA amplicon sequencing for microbial abundance and (B) time-course of crude glycerol consumption used during the fed-batch. Yellow panels indicate nitrogen limitation. Values represent the mean and standard deviation from two independent bioreactor experiments.

https://doi.org/10.1021/acssuschemeng.5c03946
ACS Sustainable Chem. Eng. XXXX, XXX, XXX−XXX

organisms at the end of the fed-batch process, where *Pseudomonas* accounted for more than 99.5% of the reads, with the remained assigned to the genus *Klebsiella*. The high-cell-density achieved by the MPC6 strain together with the pulse-wise crude glycerol feeding likely conferred a competitive advantage to the Antarctic strain (Figure 6A), rendering the fed-batch environment more restrictive to competitor than in the open batch bioreactors, which showed a slightly higher proportion of *Klebsiella* spp. (Figure 4B).

Few studies have explored the use of industrial crude glycerol as the sole carbon substrate for PHAs production in *Pseudomonas* species. Recently, an engineered *P. putida* strain overexpressing the *phaC2* and *phaG* genes along with deleting the *phaC1ZC2* operon was reported to produce 49.5 g L^{-1} of *mcl*-PHA in a fed-batch bioreactor over 180 h, resulting in a PHA productivity of 0.28 g L^{-1} h^{-1}.[18] In this regard, the maximum PHA productivity obtained in our study surpasses that of previously reported engineered *P. putida* strains under axenic conditions by nearly 2-fold.[16,18,52] This points to the importance of selecting the most appropriate feeding strategy for producing an intracellular polymer, particularly when the target product is not directly coupled to bacterial growth.[2]

Beyond performance, nonsterile NaCl-selective bioprocesses bring several advantages. They eliminate sterilization-in-place (SIP) of media and vessels, allowing operations without air filtration, which in turn reduces steam, water, filtration consumables, and electricity. These parameters can account for a substantial fraction (20−40%) of the energy costs of microbial chemical production.[9,53] It also shortens the runs between cycles because the vessels and bioreactors are simple washed rather than sterilized. Our findings that feeding nonsterile crude glycerol in an open bioreactor creates a more favorable environment for PHA synthesis by *P. frigusceleri* (Figure 4, 5), outlines a practical path to lower OPEX and CAPEX. Although oxygen-enriched air was used for 10 h during the exponential-feeding phase, this oxygen demand is a limitation that should be mitigated. One option is to reduce the imposed μ_{set}, which decreases the feeding rate along with the cellular oxygen demand. There is a tradeoff between longer runs and a decrease in PHA productivity, with a direct impact on process economics. Modeling an optimization of the feed rate and oxygen uptake rate (OUR) can identify operating points that preserve the economic advantages of nonsterile operation.

The monomer composition of the purified PHA bioproduced by *P. frigusceleri* was analyzed by GC-MS at 46 and 52 h cultivation from the fed-batch bioreactor for comparison. The biopolymers exhibited nearly identical monomeric signatures with 3HB being the main monomer in the polymeric chain (accounting for more than 87%), while the other monomers corresponded to *mcl*-PHAs (Table 3). NMR analysis was also conducted to confirm the findings obtained from GC-MS analysis. We also conducted NMR analyses (Supporting Information), which revealed that a predominantly PHB composition (∼89%) along with a minor fraction (∼11%) of *mcl*-PHA. The ^{13}C NMR spectrum confirms the presence of 3-hydroxydecanoate as the main *mcl*-PHA monomer. Additionally, smaller peaks are observed in the ^{13}C NMR spectrum within the 20−35 ppm region, indicating the presence of other shorter monomers in lower proportions than 3-hydroxydecanoate.[54,55]

The melting temperatures and the crystallization and glass transition temperatures of purified PHAs obtained after 46 and 52 h of cultivation in the fed-batch bioreactors, were relatively similar (Table 3). The biosynthesized PHA displayed a distinct glass transition temperature of 3.1 °C and a unique crystallization temperature of 55.1 °C (Table 3, Supporting Information), a common pattern of a mixture of PHB and *mcl*-PHAs. Interestingly, the average-molecular weight of PHAs decreased from 633 kDa at 46 h to 348 kDa at 52 h. However, the PDI values of PHAs remained nearly constant over time (Table 3). These results suggest that the Mw of the biosynthesized PHA can change once the maximum biopolymer accumulation capacity of *P. frigusceleri* MPC6 is reached. Consistent with our observations, previous studies have reported fluctuations in molecular weights and PDI values of homopolymers and copolymers of *short*- and *medium*-chain length PHA over time.[50,56] Such variations can affect the processing of biodegradable PHAs,[57] but the PHA produced by *P. frigusceleri* maintained a PDI close to 2 (Table 3), an advantage for polymer extrusion processes.[58]

CONCLUSIONS

This study demonstrates that the extremophile *P. frigusceleri* MPC6 exhibits high adaptability to grow under saline conditions while efficiently metabolizing crude glycerol without losing its ability to synthesize PHA. Compared to other *Pseudomonas* strains, *P. frigusceleri* maintained higher biomass yields and PHA production under increasing NaCl concentrations, with optimal accumulation occurring at 20 g L^{-1} NaCl. In nonsterile batch bioreactors, *P. frigusceleri* remained the dominant bacterial member of the community (>98% abundance) after 72 h of cultivation, achieving a PHA productivity of 0.03 g L^{-1} h^{-1} from crude glycerol. Moreover, a PHA volumetric productivity of 0.47 g L^{-1} h^{-1} was attained over 46 h by implementing a DO-stat feeding strategy in open fed-batch bioreactors. The PHA produced by *P. frigusceleri* was identified as a mixture of PHB (87−89%) and *mcl*-PHA (13−11%), as confirmed by GC-MS and NMR analyses. When PHA production peaked at 46 h within the fed-batch process, the biopolymer displayed a melting point of 175 °C, an average molecular weight of 633 kDa, and a PDI of 1.9. Extending the cultivation time to 52 h did not enhance PHA accumulation and reduced the *Mw* to 348 kDa, while the PDI value (2.0) remained relatively unchanged. A limitation of the present work is the use of pure oxygen during the exponential feeding phase to prevent oxygen limitation, which adds cost and operational complexity. Future efforts should focus on eliminating this requirement by operating at lower fractions of μ_{max} that could reduce the oxygen-uptake rate over time. This study reinforces the potential of novel halotolerant bacteria for cost-competitive, biodegradable PHA production while valorizing crude glycerol as a biobased chemical feedstock. It further shows that nonsterile bioprocessing is not limited to strict halophiles; halotolerant hosts can be cultivated in mildly saline media that eliminate the need for sterilization and are far less aggressive to stainless-steel vessels and piping than high-salt systems.

ASSOCIATED CONTENT

Supporting Information

The Supporting Information is available free of charge at https://pubs.acs.org/doi/10.1021/acssuschemeng.5c03946.

https://doi.org/10.1021/acssuschemeng.5c03946
ACS Sustainable Chem. Eng. XXXX, XXX, XXX−XXX

Additional experimental details and materials and methods, including photographs of the experimental setup (PDF)

AUTHOR INFORMATION

Corresponding Author

Ignacio Poblete-Castro − *Biosystems Engineering Laboratory, Department of Chemical and Bioprocess Engineering, Universidad de Santiago de Chile (USACH), Santiago 9160000, Chile;* orcid.org/0000-0001-6649-0389; Email: Ignacio.poblete.c@usach.cl

Authors

Matias Orellana-Saez − *Biosystems Engineering Laboratory, Department of Chemical and Bioprocess Engineering, Universidad de Santiago de Chile (USACH), Santiago 9160000, Chile*

Izabook Gutierrez-Urrutia − *Biosystems Engineering Laboratory, Department of Chemical and Bioprocess Engineering, Universidad de Santiago de Chile (USACH), Santiago 9160000, Chile*

Fabian Rodriguez-Oyarzo − *Biosystems Engineering Laboratory, Department of Chemical and Bioprocess Engineering, Universidad de Santiago de Chile (USACH), Santiago 9160000, Chile*

Benjamin Cordero-Jorquera − *Biosystems Engineering Laboratory, Department of Chemical and Bioprocess Engineering, Universidad de Santiago de Chile (USACH), Santiago 9160000, Chile*

Andrea Carvajal − *Departamento de Ingeniería Química y Ambiental, Universidad Técnica Federico Santa María, Santiago 9170022, Chile*

Eduardo Castro-Nallar − *Departamento de Microbiología, Facultad de Ciencias de la Salud and Centro de Ecología Integrativa (CEI), Universidad de Talca, Talca 3460000, Chile*

Cesar Saldias − *Facultad de Química y Farmacia, Pontificia Universidad Católica de Chile, 7820436 Macul, Chile*

Esteban A. Hernandez-Vargas − *Department of Mathematics and Statistical Science, University of Idaho, Moscow, Idaho 83844, United States*

Virginia Rivero-Buceta − *Polymer Biotechnology Group, Biological Research Centre Margarita Salas, Spanish National Research Council (CIB-CSIC), Madrid 28006, Spain; Interdisciplinary Platform for Sustainable Plastics towards a Circular Economy-Spanish National Research Council (SusPlast-CSIC), Madrid 28040, Spain;* orcid.org/0000-0002-5658-1997

Flavia C. Zacconi − *Interdisciplinary Platform for Sustainable Plastics towards a Circular Economy-Spanish National Research Council (SusPlast-CSIC), Madrid 28040, Spain; Institute for Biological and Medical Engineering, Schools of Engineering, Medicine and Biological Sciences, Pontificia Universidad Católica de Chile, 7820436 Santiago, Chile*

Complete contact information is available at: https://pubs.acs.org/10.1021/acssuschemeng.5c03946

Notes

The authors declare no competing financial interest.

ACKNOWLEDGMENTS

I.P.-C. acknowledges the support provided by ANID FONDECYT no. 1210332 and INACH (RG_17_19). This project also received financial support from Proyecto POSTDOC_DICYT, Codigo 092511PC_Postdoc, Vicerrectoría de Investigación, Desarrollo e Innovación de la USACH, and DICYT-USACH. A.C. thanks the support by ANID FONDECYT no. 1210032. We thank the technical assistant of the Centro de Instrumentación of Pontificia Universidad Católica de Chile through CONICYT-FONDEQUIP EQM120021.

REFERENCES

(1) Adeleye, A. T.; Odoh, C. K.; Enudi, O. C.; Banjoko, O. O.; Osiboye, O. O.; Odediran, E. T.; Louis, H. Sustainable Synthesis and Applications of Polyhydroxyalkanoates (PHAs) from Biomass. *Process Biochem.* **2020**, *96*, 174−193.

(2) Borrero-de Acuña, J. M. B.; Poblete-Castro, I. Rational Engineering of Natural Polyhydroxyalkanoates Producing Microorganisms for Improved Synthesis and Recovery. *Microbial Biotechnology* **2023**, *16*, 262−285.

(3) Choi, S. Y.; Rhie, M. N.; Kim, H. T.; Joo, J. C.; Cho, I. J.; Son, J.; Jo, S. Y.; Sohn, Y. J.; Baritugo, K.-A.; Pyo, J.; Lee, Y.; Lee, S. Y.; Park, S. J. Metabolic Engineering for the Synthesis of Polyesters: A 100-Year Journey from Polyhydroxyalkanoates to Non-Natural Microbial Polyesters. *Metab. Eng.* **2020**, *58*, 47−81.

(4) Saratale, R. G.; Cho, S.-K.; Saratale, G. D.; Kadam, A. A.; Ghodake, G. S.; Kumar, M.; Bharagava, R. N.; Kumar, G.; Kim, D. S.; Mulla, S. I. A Comprehensive Overview and Recent Advances on Polyhydroxyalkanoates (PHA) Production Using Various Organic Waste Streams. *Bioresour. Technol.* **2021**, No. 124685.

(5) Borrero-de Acuña, J. M.; Aravena-Carrasco, C.; Gutierrez-Urrutia, I.; Duchens, D.; Poblete-Castro, I. Enhanced Synthesis of Medium-Chain-Length Poly(3-Hydroxyalkanoates) by Inactivating the Tricarboxylate Transport System of Pseudomonas Putida KT2440 and Process Development Using Waste Vegetable Oil. *Process Biochem.* **2019**, 23.

(6) Borrero-de Acuña, J. M.; Gutierrez-Urrutia, I.; Hidalgo-Dumont, C.; Aravena-Carrasco, C.; Orellana-Saez, M.; Palominos-Gonzalez, N.; van Duuren, J. B. J. H.; Wagner, V.; Gläser, L.; Becker, J.; Kohlstedt, M.; Zacconi, F. C.; Wittmann, C.; Poblete-Castro, I. Channelling Carbon Flux through the Meta-Cleavage Route for Improved Poly(3-Hydroxyalkanoate) Production from Benzoate and Lignin-Based Aromatics in Pseudomonas Putida H. *Microb. Biotechnol.* **2020**, *n/a*, 2385.

(7) Salvachúa, D.; Rydzak, T.; Auwae, R.; De Capite, A.; Black, B. A.; Bouvier, J. T.; Cleveland, N. S.; Elmore, J. R.; Huenemann, J. D.; Katahira, R. Metabolic Engineering of Pseudomonas Putida for Increased Polyhydroxyalkanoate Production from Lignin. *Microb. Biotechnol.* **2020**, *13* (1), 290−298.

(8) Poblete-Castro, I.; Wittmann, C.; Nikel, P. I. Biochemistry, Genetics and Biotechnology of Glycerol Utilization in Pseudomonas Species. *Microb. Biotechnol.* **2020**, *13* (1), 32−53.

(9) Mitra, R.; Xu, T.; Xiang, H.; Han, J. Current Developments on Polyhydroxyalkanoates Synthesis by Using Halophiles as a Promising Cell Factory. *Microb. Cell Factories* **2020**, *19* (1), 1−30.

(10) Godard, T.; Zühlke, D.; Richter, G.; Wall, M.; Rohde, M.; Riedel, K.; Poblete-Castro, I.; Krull, R.; Biedendieck, R. Metabolic Rearrangements Causing Elevated Proline and Polyhydroxybutyrate Accumulation during the Osmotic Adaptation Response of Bacillus Megaterium. *Front. Bioeng. Biotechnol.* **2020**, *8*, 47.

(11) Kaur, J.; Sarma, A. K.; Jha, M. K.; Gera, P. Valorisation of Crude Glycerol to Value-Added Products: Perspectives of Process Technology. *Economics and Environmental Issues. Biotechnol. Rep.* **2020**, *27*, No. e00487.

(12) Samul, D.; Leja, K.; Grajek, W. Impurities of Crude Glycerol and Their Effect on Metabolite Production. *Ann. Microbiol.* **2014**, *64* (3), 891−898.
(13) Poblete-Castro, I.; Becker, J.; Dohnt, K.; Dos Santos, V. M.; Wittmann, C. Industrial Biotechnology of *Pseudomonas Putida* and Related Species. *Appl. Microbiol. Biotechnol.* **2012**, *93* (6), 2279−2290.
(14) Fu, J.; Sharma, P.; Spicer, V.; Krokhin, O. V.; Zhang, X.; Fristensky, B.; Cicek, N.; Sparling, R.; Levin, D. B.; Virolle, M. J. Quantitative 'Omics Analyses of Medium Chain Length Polyhydroxyalkanaote Metabolism in Pseudomonas Putida LS46 Cultured with Waste Glycerol and Waste Fatty Acids. *PLOS ONE* **2015**, *10* (11), No. e0142322.
(15) Poblete-Castro, I.; Binger, D.; Oehlert, R.; Rohde, M. Comparison of Mcl-Poly(3-Hydroxyalkanoates) Synthesis by Different Pseudomonas Putida Strains from Crude Glycerol: Citrate Accumulates at High Titer under PHA-Producing Conditions. *BMC Biotechnol.* **2014**, *14*, 962.
(16) Borrero-de Acuña, J. M.; Rohde, M.; Saldias, C.; Poblete-Castro, I. Fed-Batch Mcl- Polyhydroxyalkanoates Production in Pseudomonas Putida KT2440 and ΔphaZ Mutant on Biodiesel-Derived Crude Glycerol. *Front. Bioeng. Biotechnol.* **2021**, No. 642023.
(17) Kenny, S.; Runic, J.; Kaminsky, W.; Woods, T.; Babu, R.; O'Connor, K. Development of a Bioprocess to Convert PET Derived Terephthalic Acid and Biodiesel Derived Glycerol to Medium Chain Length Polyhydroxyalkanoate. *Appl. Microbiol. Biotechnol.* **2012**, *95* (3), 623−633.
(18) Hur, D. H.; Lee, J.; Park, S. J.; Jeong, K. J. Engineering of Pseudomonas Putida to Produce Medium-Chain-Length Polyhydroxyalkanoate from Crude Glycerol. *Int. J. Biol. Macromol.* **2024**, *281*, No. 136411.
(19) Van-Thuoc, D.; Huu-Phong, T.; Minh-Khuong, D.; Hatti-Kaul, R. Poly (3-Hydroxybutyrate-Co-3-Hydroxyvalerate) Production by a Moderate Halophile Yangia Sp. ND199 Using Glycerol as a Carbon Source. *Appl. Biochem. Biotechnol.* **2015**, *175*, 3120−3132.
(20) Pacheco, N.; Orellana-Saez, M.; Pepczynska, M.; Enrione, J.; Bassas-Galia, M.; Borrero-de Acuña, J. M.; Zacconi, F. C.; Marcoleta, A. E.; Poblete-Castro, I. Exploiting the Natural Poly(3-Hydroxyalkanoates) Production Capacity of Antarctic Pseudomonas Strains: From Unique Phenotypes to Novel Biopolymers. *J. Ind. Microbiol. Biotechnol.* **2019**, *46*, 1139.
(21) Orellana-Saez, M.; Pacheco, N.; Costa, J. I.; Mendez, K. N.; Miossec, M. J.; Meneses, C.; Castro-Nallar, E.; Marcoleta, A. E.; Poblete-Castro, I. In-Depth Genomic and Phenotypic Characterization of the Antarctic Psychrotolerant Strain Pseudomonas Sp. MPC6 Reveals Unique Metabolic Features, Plasticity, and Biotechnological Potential. 2019.
(22) Orellana-Saez, M.; Lauzurique, Y.; Donoso-Garcia, P.; Carmona, M.; Carvajal, A.; Riveros, A. L.; Kogan, M. J.; Báez, D. F.; Poblete-Castro, I. Aerobic Bioremediation of Selenite in Marine and Freshwater Environments via Intracellular Selenium Nanoparticle Formation by Pseudomonas Frigusceleri MPC6 in Glycerol-Fed Continuous Bioreactors. *J. Environ. Manage.* **2025**, *382*, No. 125370.
(23) Vizoso, P.; Pacheco, N.; Bastias-Molina, M.; Meneses, C.; Poblete-Castro, I. Draft Genome Sequence of the Phenol-Degrading Bacterium Pseudomonas Putida H. *Genome Announc* **2015**, *3* (4), No. e00936-15.
(24) Miller, J. H.*Experiments in Molecular Genetics*. No Title 1972.
(25) Beckers, V.; Poblete-Castro, I.; Tomasch, J.; Wittmann, C. Integrated Analysis of Gene Expression and Metabolic Fluxes in PHA-Producing Pseudomonas Putida Grown on Glycerol. *Microb. Cell Factories* **2016**, *15* (1), 73.
(26) Lageveen, R. G.; Huisman, G. W.; Preusting, H.; Ketelaar, P.; Eggink, G.; Witholt, B. Formation of Polyesters by Pseudomonas Oleovorans: Effect of Substrates on Formation and Composition of Poly-(R)-3-Hydroxyalkanoates and Poly-(R)-3-Hydroxyalkenoates. *Appl. Environ. Microbiol.* **1988**, *54* (12), 2924−2932.
(27) Oliva-Arancibia, B.; Ordenes-Aenishanslins, N.; Bruna, N.; Ibarra, P. S.; Zacconi, F. C.; Pérez-Donoso, J. M.; Poblete-Castro, I. Co-Synthesis of Medium-Chain-Length Polyhydroxyalkanoates and CdS Quantum Dots Nanoparticles in Pseudomonas Putida KT2440. *J. Biotechnol.* **2017**, 29.
(28) Walters, W.; Hyde, E. R.; Berg-Lyons, D.; Ackermann, G.; Humphrey, G.; Parada, A.; Gilbert, J. A.; Jansson, J. K.; Caporaso, J. G.; Fuhrman, J. A.; Apprill, A.; Knight, R. Improved Bacterial 16S rRNA Gene (V4 and V4−5) and Fungal Internal Transcribed Spacer Marker Gene Primers for Microbial Community Surveys. *mSystems* **2016**, *1* (1), No. e00009-15.
(29) Comeau, A. M.; Douglas, G. M.; Langille, M. G. I. Microbiome Helper: A Custom and Streamlined Workflow for Microbiome Research. *mSystems* **2017**, *2* (1), No. e00127.
(30) Callahan, B. J.; McMurdie, P. J.; Rosen, M. J.; Han, A. W.; Johnson, A. J. A.; Holmes, S. P. DADA2: High-Resolution Sample Inference from Illumina Amplicon Data. *Nat. Methods* **2016**, *13* (7), 581−583.
(31) Mykytczuk, N. C. S.; Foote, S. J.; Omelon, C. R.; Southam, G.; Greer, C. W.; Whyte, L. G. Bacterial Growth at − 15 °C; Molecular Insights from the Permafrost Bacterium Planococcus Halocryophilus Or1. *ISME J.* **2013**, *7* (6), 1211−1226.
(32) Lipson, D. A. The Complex Relationship between Microbial Growth Rate and Yield and Its Implications for Ecosystem Processes. *Front. Microbiol.* **2015**, *6*, No. 615.
(33) Passanha, P.; Kedia, G.; Dinsdale, R. M.; Guwy, A. J.; Esteves, S. R. The Use of NaCl Addition for the Improvement of Polyhydroxyalkanoate Production by Cupriavidus Necator. *Bioresour. Technol.* **2014**, *163*, 287−294.
(34) Mozumder, M. S. I.; Garcia-Gonzalez, L.; De Wever, H.; Volcke, E. I. P. Effect of Sodium Accumulation on Heterotrophic Growth and Polyhydroxybutyrate (PHB) Production by Cupriavidus Necator. *Bioresour. Technol.* **2015**, *191*, 213−218.
(35) Hong, J.-W.; Song, H.-S.; Moon, Y.-M.; Hong, Y.-G.; Bhatia, S. K.; Jung, H.-R.; Choi, T.-R.; Yang, S.; Park, H.-Y.; Choi, Y.-K.; Yang, Y.-H. Polyhydroxybutyrate Production in Halophilic Marine Bacteria Vibrio Proteolyticus Isolated from the Korean Peninsula. *Bioprocess Biosyst. Eng.* **2019**, *42* (4), 603−610.
(36) Zhang, J.; Yan, X.; Park, H.; Scrutton, N. S.; Chen, T.; Chen, G.-Q. Nonsterile Microbial Production of Chemicals Based on Halomonas Spp. *Curr. Opin. Biotechnol.* **2024**, *85*, No. 103064.
(37) Cox-Fermandois, A.; Berríos-Pastén, C.; Serrano, C.; Arros, P.; Poblete-Castro, I.; Marcoleta, A. Large-Scale Analysis of Polyhydroxyalkanoate Synthases in Pseudomonas: Highly Diverse Enzymes with Potential for a Novel Class and Dissemination by Horizontal Gene Transfer. *J. Appl. Microbiol.* **2025**, *136* (8), No. lxaf179.
(38) Ma, Jiangshan; Jiang, Huan; Hector, Stanton B.; Xiao, Zhihong; Li, Jilie; Liu, Rukuan; Li, Changzhu; Zeng, Baiquan; Liu, Gao-Qiang; Zhu, Yonghua Adaptability of Klebsiella Pneumoniae 2e, a Newly Isolated 1,3-Propanediol-Producing Strain, to Crude Glycerol as Revealed by Genomic Profiling. *Appl. Environ. Microbiol.* **2019**, *85* (10), No. e00254−19.
(39) Moon, C.; Ahn, J.-H.; Kim, S. W.; Sang, B.-I.; Um, Y. Effect of Biodiesel-Derived Raw Glycerol on 1, 3-Propanediol Production by Different Microorganisms. *Appl. Biochem. Biotechnol.* **2010**, *161*, 502−510.
(40) Kratz, J. C.; Banerjee, S. Dynamic Proteome Trade-Offs Regulate Bacterial Cell Size and Growth in Fluctuating Nutrient Environments. *Commun. Biol.* **2023**, *6* (1), 486.
(41) Dai, X.; Zhu, M. High Osmolarity Modulates Bacterial Cell Size through Reducing Initiation Volume in Escherichia Coli. *mSphere* **2018**, *3* (5), 10-1128.
(42) Parsons, J. B.; Rock, C. O. Bacterial Lipids: Metabolism and Membrane Homeostasis. *Prog. Lipid Res.* **2013**, *52* (3), 249−276.
(43) Reva, O. N.; Weinel, C.; Weinel, M.; Böhm, K.; Stjepandic, D.; Hoheisel, J. D.; Tümmler, B. Functional Genomics of Stress Response in Pseudomonas Putida KT2440. *J. Bacteriol.* **2006**, *188* (11), 4079−4092.
(44) Eberlein, C.; Baumgarten, T.; Starke, S.; Heipieper, H. J. Immediate Response Mechanisms of Gram-Negative Solvent-Tolerant Bacteria to Cope with Environmental Stress: Cis-Trans Isomerization of Unsaturated Fatty Acids and Outer Membrane

https://doi.org/10.1021/acssuschemeng.5c03946
ACS Sustainable Chem. Eng. XXXX, XXX, XXX−XXX

Vesicle Secretion. *Appl. Microbiol. Biotechnol.* **2018**, *102* (6), 2583−2593.
(45) Choi, T.-R.; Park, Y.-L.; Song, H.-S.; Lee, S. M.; Park, S. L.; Lee, H. S.; Kim, H.-J.; Bhatia, S. K.; Gurav, R.; Lee, Y. K.; Sung, C.; Yang, Y.-H. Effects of a Δ-9-Fatty Acid Desaturase and a Cyclopropane-Fatty Acid Synthase from the Novel Psychrophile Pseudomonas Sp. B14−6 on Bacterial Membrane Properties. *J. Ind. Microbiol. Biotechnol.* **2020**, *47* (12), 1045−1057.
(46) Hachicho, N.; Birnbaum, A.; Heipieper, H. J. Osmotic Stress in Colony and Planktonic Cells of Pseudomonas Putida Mt-2 Revealed Significant Differences in Adaptive Response Mechanisms. *AMB Express* **2017**, *7* (1), 62.
(47) Bengtsson, S.; Pisco, A. R.; Johansson, P.; Lemos, P. C.; Reis, M. A. M. Molecular Weight and Thermal Properties of Polyhydroxyalkanoates Produced from Fermented Sugar Molasses by Open Mixed Cultures. *J. Biotechnol.* **2010**, *147* (3), 172−179.
(48) Murugan, P.; Gan, C.-Y.; Sudesh, K. Biosynthesis of P(3HB-Co-3HHx) with Improved Molecular Weights from a Mixture of Palm Olein and Fructose by Cupriavidus Necator Re2058/pCB113. *Int. J. Biol. Macromol.* **2017**, *102*, 1112−1119.
(49) Oh, S.-J.; Kim, S.; Lee, Y.; Shin, Y.; Choi, S.; Oh, J.; Bhatia, S. K.; Joo, J. C.; Yang, Y.-H. Controlled Production of a Polyhydroxyalkanoate (PHA) Tetramer Containing Different Mole Fraction of 3-Hydroxybutyrate (3HB), 3-Hydroxyvalerate (3 HV), 4 HV and 5 HV Units by Engineered Cupriavidus Necator. *Int. J. Biol. Macromol.* **2024**, *266*, No. 131332.
(50) Budde, Charles F.; Riedel, Sebastian L.; Willis, Laura B.; Rha, ChoKyun; Sinskey, Anthony J. Production of Poly(3-Hydroxybutyrate-Co-3-Hydroxyhexanoate) from Plant Oil by Engineered Ralstonia Eutropha Strains. *Appl. Environ. Microbiol.* **2011**, *77* (9), 2847−2854.
(51) Poblete-Castro, I.; Rodriguez, A.; Lam, C.; Kessler, W. Improved Production of Medium-Chain-Length Polyhydroxyalkanoates in Glucose-Based Fed-Batch Cultivations of Metabolically Engineered Pseudomonas Putida Strains. *J. Microbiol. Biotechnol.* **2014**, *24* (1), 59−69.
(52) Borrero-de Acuña, J. M.; Hidalgo-Dumont, C.; Pacheco, N.; Cabrera, A.; Poblete-Castro, I. A Novel Programmable Lysozyme-Based Lysis System in Pseudomonas Putida for Biopolymer Production. *Sci. Rep.* **2017**, *7* (1), 4373.
(53) Li, T.; Chen, X.; Chen, J.; Wu, Q.; Chen, G.-Q. Open and Continuous Fermentation: Products, Conditions and Bioprocess Economy. *Biotechnol. J.* **2014**, *9* (12), 1503−1511.
(54) Tripathi, L.; Wu, L.-P.; Chen, J.; Chen, G.-Q. Synthesis of Diblock Copolymer Poly-3-Hydroxybutyrate -Block-Poly-3-Hydroxyhexanoate [PHB-b-PHHx] by a β-Oxidation Weakened Pseudomonas Putida KT2442. *Microb. Cell Factories* **2012**, *11* (1), No. 44.
(55) Ortiz, R.; Basnett, P.; Roy, I.; Quintana, I. Picosecond Laser Ablation of Polyhydroxyalkanoates (PHAs): Comparative Study of Neat and Blended Material Response. *Polymers* **2020**, *12* (1), 127.
(56) Arikawa, H.; Sato, S.; Fujiki, T.; Matsumoto, K. A Study on the Relation between Poly(3-Hydroxybutyrate) Depolymerases or Oligomer Hydrolases and Molecular Weight of Polyhydroxyalkanoates Accumulating in Cupriavidus Necator H16. *J. Biotechnol.* **2016**, *227*, 94−102.
(57) Garcia-Garcia, D.; Quiles-Carrillo, L.; Balart, R.; Torres-Giner, S.; Arrieta, M. P. Innovative Solutions and Challenges to Increase the Use of Poly(3-Hydroxybutyrate) in Food Packaging and Disposables. *Eur. Polym. J.* **2022**, *178*, No. 111505.
(58) Debuissy, T.; Pollet, E.; Avérous, L. Synthesis and Characterization of Block Poly(Ester-Ether-Urethane)s from Bacterial Poly(3-Hydroxybutyrate) Oligomers. *J. Polym. Sci. Part Polym. Chem.* **2017**, *55* (11), 1949−1961.

NOTE ADDED AFTER ASAP PUBLICATION

Due to a production error, this paper was published ASAP on September 29, 2025, with an older version of the TOC/abstract graphic. The corrected version was reposted on September 30, 2025.

https://doi.org/10.1021/acssuschemeng.5c03946
ACS Sustainable Chem. Eng. XXXX, XXX, XXX−XXX